

---

## RESEARCH NOTE

---

# THREE-DIMENSIONAL SIMULATION OF AIRFLOW AND NANO-PARTICLE BEAM FOCUSING IN AERODYNAMIC LENSES

*Omid. Abouali\**

*Department of Mechanical Engineering, Shiraz University  
Shiraz, Iran  
abouali@shirazu.ac.ir*

*Goodarz. Ahmadi*

*Department of Mechanical and Aeronautical Engineering, Clarkson University  
Potsdam, NY, 13699-5725  
ahmadi@clarkson.edu*

\*Corresponding Author

(Received: March 1, 2005 – Accepted in Revised Form: January 18, 2007)

**Abstract** In this paper airflow, nano- and micro-particle motions in an aerodynamic particle beam focusing system consisting of several lenses, a nozzle and the downstream chamber, was studied. A three - dimensional numerical simulation for the system was presented and the compressible airflow and thermal conditions in the aerodynamic lens system were evaluated. Dilute particle concentration was assumed so that the particle motion does not affect the flow field and a one-way coupling is assumed. In the computational model, an intermediate chamber with different size skimmers downstream of the nozzle was also considered. The simulation results for 3-dimensional flow field showed that the assumption of axi-symmetric flow is reasonable at the downstream of the nozzle. The performance of the lens with air as carrier gas for focusing nano- and micro- particles was discussed. The results showed that the sub 30 nm particle trajectories are three - dimensional and the assumption of the axi-symmetric particle motions is not valid.

**Keywords** Aerodynamic, Lenses, Nano, Micro, Particles

**چکیده** در این مقاله جریان هوا و حرکت ذرات در سائز میکرو و نانو در یک سیستم لنز ایرودینامیک مورد مطالعه قرار می‌گیرد. این سیستم شامل چندین لنز، نازل و نیز محفظه میانی پائین دست نازل می‌باشد و به منظور متمرکزسازی ذرات به صورت یک پرتو باریک به کار می‌رود. به منظور مطالعه جریان تراکم‌پذیر در درون این سیستم یک مدل سه بعدی کامپیوتری تهیه شده است. با توجه به غلظت سیستم ذرات در جریان هوا، فرض شده است که حرکت ذرات بر روی جریان تأثیری نمی‌گذارد، بدین خاطر ابتدا میدان جریان از دیدگاه اولرین و سپس معادلات مربوط به حرکت ذرات از دیدگاه لاگرانژین مورد بررسی قرار گرفته است. نتایج نشان‌دهنده این است که فرض جریان متقارن محوری برای جریان هوا در پایین دست نازل قابل قبول می‌باشد. عملکرد لنز ایرودینامیک با هوا به عنوان گاز حامل برای متمرکزسازی ذرات میکرو و نانو مورد بحث قرار گرفته است. نتایج نشان‌دهنده این است که مسیر حرکت ذرات برای ذرات با قطر کوچکتر از ۳۰ نانومتر سه بعدی بوده و فرض حرکت ذرات بصورت متقارن محوری که تا بحال در تحقیقات گذشته استفاده شده است قابل قبول نمی‌باشد.

## 1. INTRODUCTION

Aerodynamic lenses are used for generating focused particle beams. These lenses are formed by

combinations of properly designed axi-symmetric contractions and expansions. Particles in a critical size range passing through a sequence of contractions drift towards the axis and form a

narrow beam. Particles larger than the critical size range are removed from the stream by inertial impaction on the lens wall, while smaller particles follow the flow streamlines and are not focused. The diameter of the focused particle beam can be controlled with a set of lenses of varying contraction diameters.

One important application of the aerodynamic lenses is to produce focused aerosol particle beam for online characterization of fine particles [1-4]. Murphy and Sears [5] reported producing narrow particle beams by expanding an aerosol from atmospheric pressure to low backpressures through a nozzle. Various nozzle types such as capillary, conically convergent, and plate orifice were used by a number of researchers [6-12] (Dahneke and Cheng [6-7]; Estes et al. [8]; Fernandez de la Mora and Rieso-Chueca [9]; Israel and Friedlander [10]; Mallina et al. [11]; Middha and Wexler [12]). Highly converging nozzles produce a small beam diameter at a focal point close to the nozzle exit, but produce a highly divergent beam downstream from the nozzle. The beams generated by gradually convergent and capillary nozzles, however, have smaller diameters that can be sustained for larger distances. Mallina et al. [11] showed that generally a narrow beam diameter generated by a nozzle is limited to a very small range of particle diameters.

Particle beam focusing can also be achieved by using sheath gas. Sheath gas reduces particle velocity and particle beam diameters. Sheath gas is normally added upstream of the nozzle in the radial direction which brings the particles toward the axis. As particles get closer to the axis, they experience less radial drag force, which in turn results in a narrow focused beam downstream of the nozzle. Dahneke and Cheng [6-7] showed that using sheath airflow at a rate which is approximately equal to the inlet flow rate the particles beam diameter could be reduced by a factor of ten. Rao et al. [13] and Kievit et al. [14] investigated the effect of sheath air on the particle beam characteristics. Using the sheath air, however, dilutes the particle concentration and requires an additional air-handling component.

Another way of generating a focused particle beam is using aerodynamic lenses. These lenses are formed by combining a series of axi-symmetric

contractions and expansions focusing elements. Computational and experimental studies of aerodynamic lenses were first performed by Liu et al. [15-16]. They showed that highly collimated particle beams could be produced without sheath air. In general, particles in a critical size range passing through a contraction drift towards the axis, and by using a number of aerodynamic lenses in the series, the particles can be collimated to form a focused beam. Liu et al. [15] evaluated the flow field in the lens and attached the nozzle using both incompressible and compressible axi-symmetric Navier-Stokes equations and a one-dimensional empirical correlation for flows downstream of the nozzle. The energy equation however was not solved and an isentropic assumption was used to relate the gas temperature to pressure. They also investigated the effect of the Brownian motion and the lift force on the particle beam diameter downstream of the nozzle. They assumed a correlation for the quasi one - dimensional flow downstream of the nozzle, which relates the Mach number of the flow to the distance from the nozzle exit. Absence of a multidimensional gas velocity field reduces the accuracy of their particle trajectory analysis especially away from the axis. In their computational model, Liu et al. [15] ignored effects of the impaction of large particles on the lens wall.

Jayne et al. [1] developed an aerosol mass spectrometer with a combination of aerodynamic lenses, which focused the particles into a narrow beam. They also studied the performance of the aerodynamic lens using the FLUENT software. Jayne et al. [1] used a design similar to the inlet system of Liu et al. [15-16] but with a hot surface followed by an electron impact ionization device and quadruple mass spectrometer. These allowed for the real - time analysis of size resolved particle mass and chemical compositions. The work of Jayne et al. [1] was limited to the modeling of the flow and particle motions inside the aerodynamic lenses up to the nozzle exit.

Zhang et al. [2] characterized particle beam collimation in a single aerodynamic lens and an individual nozzle using the FLUENT software. They found that the maximum particle displacement and particle loss occurs at a particle Stokes number near unity. The performance

characteristics of the lens and the nozzle were found to depend on their geometry, their flow Reynolds number, and also their particle Stokes number.

Using FLUENT™ software, Abouali and Ahmadi [17] studied axi-symmetric airflow and particle motions in multistage aerodynamic lenses with an intermediate chamber. In addition to the gas flow field and particle trajectory inside the lens, the gas flow downstream of the nozzle in the intermediate chamber was also analyzed. Suitability of different assumptions for the slip correction was examined and it was shown that the Stokes - Cunningham expression with the variable Cunningham correction factor is reasonably accurate for performance analysis of aerodynamic lenses. It was also shown that the effects of the lift and thermophoresis forces are negligible. The simulation results showed that for particles in the size range between 50 to 1000 nm, a focusing efficiency of more than 97 % could be achieved. The collection efficiency for larger particles, however, decreases somewhat due to the inertial impact effects in the focusing elements. For smaller particles (less than 30 nm), the collection efficiency also decreases due to Brownian motion effects.

Using FLUENT™, Zhang et al. [18] studied the gas - particle flows through an integrated aerodynamic - lens - nozzle. They found that the inlet transmission efficiency ( $\eta_i$ ) for particles of intermediate diameters ( $D_p \sim 30\text{-}500$  nm) was about unity. The transmission efficiency gradually reduced to about 40 % for large particles with  $D_p > 2500$  nm. Their result also showed that there was a significant reduction of  $\eta_i$  to almost zero for very small particles with  $D_p \leq 15$  nm because these particles faithfully follow the final gas expansion.

Wang et al. [19] developed a numerical simulation methodology that was able to accurately characterize the focusing performance of aerodynamic lens systems. They used the FLUENT™ code for simulating the gas flow field and the particle motions. Particle trajectories were tracked using the Lagrangian approach of the code and Brownian motion of nano-particles and which was incorporated in their numerical simulations. They demonstrated the ability of aerodynamic lenses to focus sub- 30 nm spherical unit density

particles. They developed a user defined subroutine for accurate modelling of the Brownian motion.

All earlier computational modeling studies of aerodynamic lenses were restricted to the assumption of the axi-symmetric flow and particle trajectories. Axi-symmetric particle motion is generally questionable since the Brownian motion is generated by three-dimensional stochastic excitations. The asymmetry in trajectories is clearly noticeable for nano-particles. In this study a three - dimensional computer model for the flow field and particle motion in aerodynamic lenses was developed. For evaluating the flow field in the aerodynamic lens and its downstream chamber, the software program FLUENT™ version 6 was used. The code does not provide the appropriate correction to the drag force for extremely low and highly variable pressure fields. Therefore, the code was augmented with the addition of user - defined subroutines for including the appropriate correction to the drag force.

## 2. MODEL DESCRIPTION

The aerodynamic lens system used by Liu et al. [16] consists of multistage focusing lens, an outlet nozzle, an intermediate chamber, and a detection chamber. A three-dimensional view of the aerodynamic lens system including the intermediate chamber is shown in Figure 1. In this paper a 3-D computational model was employed to study this aerodynamic lens system.

The diameter of the lens tube is 10 mm and adjacent focusing elements are located 50 mm apart. The contraction diameters of the five lenses that are used in the analysis are 5.0, 4.5, 4.0, 3.75, 3.5 mm, respectively. At the end of the five focusing elements, the gas passes through a nozzle with a diameter of 6 mm. In the experimental work of Liu et al. [16], the flow expands in the aerodynamic focusing elements and the nozzle into a low-pressure intermediate chamber, which is kept at about 10 Pa. A vacuum pump is attached to the intermediate chamber to remove a significant amount of gas from the stream. Focused particles and a small amount of gas pass through a skimmer into a very low- pressure detection chamber. The

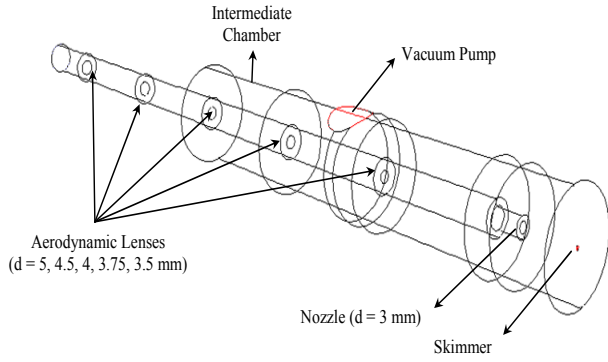


**Figure 1.** Schematics of the aerodynamic lens system.

detection chamber is kept at a pressure of about 0.1 Pa. Particles are captured on a plate at the end of the detection chamber.

The mean free path of the gas in the detection chamber is of the order of chamber size; thus, the continuum flow assumption can not be used for this region. The flow in the lens and the nozzle is roughly axi-symmetric, however, due to the presence of the vacuum pump exhaust, the flow in the chamber is not axi-symmetric. The gas flow in the intermediate chamber downstream of the nozzle with  $\lambda/L = 0.1$ , however, may be treated as being in the continuum regime.

### 3. GOVERNING EQUATIONS

**3.1. Gas Flow Governing Equations** For a dilute gas - particle flow in an aerodynamic lens, a one - way interaction model is used. That is, it is assumed while gas will carry the particles, the concentration and size of the particles are too small to affect the gas flow. Under this condition the gas flow field can first be evaluated and then be used for evaluation of particle trajectories. The maximum Reynolds number is related to the exiting flow of the nozzle and is nearly equal to 50. The three-dimensional compressible viscous laminar flow field in the lens and intermediate chamber was evaluated using FLUENT software. Navier-Stokes equations in Cartesian coordinates, in the conservative form are:

$$Q_t + (E - E_v)_x + (F - F_v)_y + (G - G_v)_z = 0 \quad (1)$$

$$Q = \begin{bmatrix} e \\ \rho \\ \rho u \\ \rho v \\ \rho w \end{bmatrix} \quad E = \begin{bmatrix} (e+p)u \\ \rho u \\ \rho u^2 + p \\ \rho uv \\ \rho uw \end{bmatrix} \quad F = \begin{bmatrix} (e+p)v \\ \rho v \\ \rho v^2 + p \\ \rho v^2 + p \\ \rho vw \end{bmatrix} \quad G = \begin{bmatrix} (e+p)w \\ \rho w \\ \rho uw \\ \rho vw \\ \rho w^2 + p \end{bmatrix} \quad (2)$$

$$E_v = \begin{bmatrix} u\tau_{xx} + v\tau_{xy} + w\tau_{xz} - q_x \\ 0 \\ \tau_{xx} \\ \tau_{xy} \\ \tau_{xz} \end{bmatrix} \quad F_v = \begin{bmatrix} u\tau_{yx} + v\tau_{yy} + w\tau_{yz} - q_y \\ 0 \\ \tau_{yx} \\ \tau_{yy} \\ \tau_{yz} \end{bmatrix} \quad G_v = \begin{bmatrix} u\tau_{zx} + v\tau_{zy} + w\tau_{zz} - q_z \\ 0 \\ \tau_{zx} \\ \tau_{zy} \\ \tau_{zz} \end{bmatrix} \quad (3)$$

In which:

$$e = \frac{p}{\gamma - 1} + \frac{\rho}{2}(u^2 + v^2 + w^2) \quad (4)$$

$$\tau_{xx} = \frac{2}{3}\mu \left( 2\frac{\partial u}{\partial x} - \frac{\partial v}{\partial y} - \frac{\partial w}{\partial z} \right), \tau_{yy} = \frac{2}{3}\mu \left( 2\frac{\partial v}{\partial y} - \frac{\partial u}{\partial x} - \frac{\partial w}{\partial z} \right) \\ \tau_{zz} = \frac{2}{3}\mu \left( 2\frac{\partial w}{\partial z} - \frac{\partial u}{\partial x} - \frac{\partial v}{\partial y} \right), \tau_{xy} = \tau_{yx} = \mu \left( \frac{\partial u}{\partial y} + \frac{\partial v}{\partial x} \right) \\ \tau_{yz} = \tau_{zy} = \mu \left( \frac{\partial v}{\partial z} + \frac{\partial w}{\partial y} \right), \tau_{xz} = \tau_{zx} = \mu \left( \frac{\partial u}{\partial z} + \frac{\partial w}{\partial x} \right) \quad (5)$$

$$q_x = -k \frac{\partial T}{\partial x} \quad q_y = -k \frac{\partial T}{\partial y} \quad q_z = -k \frac{\partial T}{\partial z} \quad (6)$$

The coefficient of viscosity and thermal conductivity have been related to the thermodynamic variables using the kinetic theory. The Sutherland's formula for viscosity is given by:

$$\mu = C_1 \frac{T^{\frac{3}{2}}}{T + C_2} \quad (7)$$

where  $C_1$  and  $C_2$  are constants for a given gas. For air at moderate temperatures,  $C_1 = 1.458 \times 10^{-6}$  kg/ms (K)<sup>1/2</sup> and  $C_2 = 110.4$ K. The Prandtl number  $Pr = C_p \mu / k$  is often used to determine the coefficient of thermal conductivity.

The numerical solution is converged if the residual decreases less than a desired small number. The residual computed by FLUENT solver is the imbalance in each discretized equation summed over all the computational cells. In this study, the iterative solution was continued until all equations' residual decreased less than  $10^{-6}$ .

**3.2. Particle Equation of Motion** The Lagrangian equation of the motion of a particle is given as

$$\frac{d V_p}{d t} = F_D + F_B - g \frac{(\rho_p - \rho)}{\rho_p} \vec{j}, \quad (8)$$

where  $V_p$  is the particle velocity vector,  $F_D$  is the drag force per unit mass,  $F_B$  is the Brownian force per unit mass,  $g$  is the acceleration of gravity,  $\vec{j}$  is the unit vector in  $y$  direction of Cartesian coordinates,  $\rho$  is the gas density, and  $\rho_p$  is the particle density. Abouali and Ahmadi [17] showed that the lift and thermophoresis forces are negligible for this application.

**3.3. Drag Force** For small particles, the Stokes - Cunningham drag, which includes the Cunningham correction to the Stokes drag force, is commonly used in the aerosol literature [20].

$$F_D = \frac{3\mu D_p Re}{4\rho_p D_p^2 C_c} (v - V_p), \quad (9)$$

Where  $V$  is the fluid velocity vector,  $D_p$  is the particle diameter,  $\mu$  is the coefficient of viscosity, and  $C_c$  is the Cunningham correction factor given as [20],

$$C_c = 1 + \frac{2\lambda}{d_p} \left[ 1.257 + 0.4 \exp \left( -1.1 \left( \frac{d_p}{2\lambda} \right) \right) \right] \quad (10)$$

In Equation 9, the Reynolds number is defined as

$$Re = \frac{|V - V_p| d_p}{\nu}, \quad (11)$$

Where  $\nu$  is the gas kinematic viscosity and  $C_D$  is the drag coefficient [20],

$$C_D = \frac{24}{Re} (1 + 0.15 Re^{0.687}) \quad (12)$$

The Cunningham correction factor given by Equation 10 depends on the gas mean free path and thus is a function of the local temperature and pressure. As noted by Abouali and Ahmadi [17,21] and Wang et al. [19] for the flow in which the gas pressure under goes large variations, use of a constant Cunningham correction factor is not acceptable. In this study, the Stokes-Cunningham expression of the drag force with a variable Cunningham correction factor is used. The Cunningham correction factor is evaluated at every point of the flow field as a function of local mean free path. The mean free path as a function of local temperature and pressure is given as [22],

$$\lambda = \frac{0.031 T^{1.3}}{P} \quad (13)$$

Here  $\lambda$  is in  $\mu\text{m}$ , pressure is in mm Hg, and temperature is in degrees Kelvin.

Since the FLUENT code does not accommodate for a variable Cunningham correction factor, a user-defined subroutine was developed and Equations 10 with variable gas mean free path were included in the analysis.

**3.4. Brownian Effects** Small particles are subjected to random impact of gas molecules that leads to their Brownian motion. In the

computational model, the Brownian motion of the particle was included in the analysis by addition of an appropriate Gaussian white noise excitation to the equation of motion. The spectral intensity  $S_{n,ij}$  given by Li and Ahmadi [23-24],

$$S_{n,ij} = S_o \delta_{ij} \quad (14)$$

Where  $\delta_{ij}$  is the Kronecker delta function, and

$$S_o = \frac{216\nu\sigma T}{\pi^2 \rho d_p^5 \left(\frac{\rho_p}{\rho}\right)^2 C_c} \quad (15)$$

T is the absolute temperature of the fluid,  $\nu$  is the kinematic viscosity, and  $\sigma$  is the Stefan - Boltzmann constant. Amplitudes of the Brownian force components are of the form

$$F_{bi} = \xi_i \sqrt{\frac{\pi S_o}{\Delta t}} \quad (16)$$

where  $\xi_i$  are zero-mean, unit-variance-independent Gaussian random numbers. The amplitudes of the Brownian force components are evaluated at each time step.

FLUENT by default uses a constant slip factor in the Brownian force calculation and this is one of the limitations of our work. We set the constant based on the nozzle upstream properties of the flow field, because the Brownian motion is more important in this region compared with intermediate chamber in which the pressure is very low.

#### 4. RESULTS

Using a computational modeling approach the flow fields in a class of aerodynamic lenses are simulated for the experimental conditions of Liu et al. [16]. Liu et al. used two different geometries in the experiments, which are studied in this section. In the first case, where the skimmer diameter was 7 mm, the distance between the nozzle and the skimmer was 10 mm (henceforth to be called as larger skimmer). In the second case, the skimmer

diameter was 1 mm and the distance between the nozzle and the skimmer was 20 mm. This case will be referred to as the small skimmer lens.

A grid study was done to find a flow field solution independent of the grid sizes. Grids with different numbers, stream wise, in radial and circumferential directions are used. Based on this study, more attention should be given to the downstream of the nozzle, so a computational grid with a number of 120000 elements locally adapted in the supersonic free jet downstream of the nozzle was used for simulating gas flow in the 3-D model of aerodynamic lens including the intermediate chamber. The grid is shown in Figure 2.

A mass flow rate boundary condition at the inlet of the aerodynamic lens was used. Fixed pressure boundary conditions were imposed at the skimmer and at the exit to the vacuum pump.

In the experimental study of Liu et al. [16] the pressure upstream of the lenses was 300 Pa, the pressure in the intermediate chamber was 10 Pa and the pressure in the detection chamber was 0.1 Pa (near vacuum). The flow in the detection chamber is clearly in a non - continuum flow regime because of the large Knudson number (large gas mean free path) with  $K_n = 2\lambda/L \sim 20$ . The flow in the intermediate chamber with  $\lambda/L \sim 0.1$ , however, is in a nearly continuum regime.

The Mach contours distributions are shown in Figures 3. These figures show that the flow expands to the Mach number of about 1.9 in the intermediate chamber. The Mach number at the nozzle exit is slightly less than 1 because of the wall boundary layer effect and has a variation across the section. This is in contrast with the common assumptions used in the earlier studies in

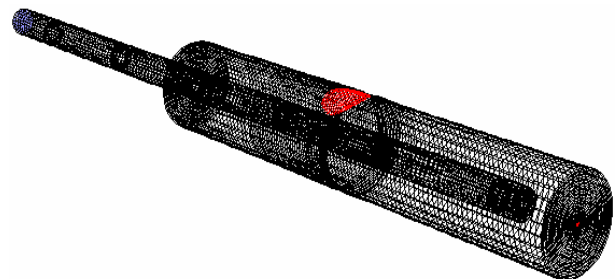
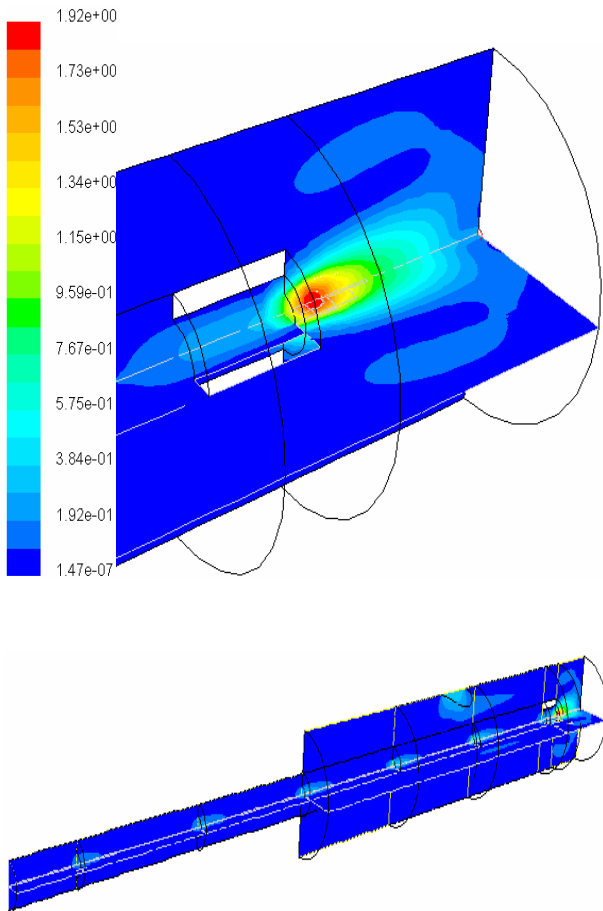


Figure 2. Schematics of the computational grid.



**Figure 3.** Mach contours for the small skimmer case.

which the intermediate chamber was not considered. Afterward it shows an axi - symmetric behavior for the flow field downstream of the nozzle.

To emphasize on the axi-symmetric behavior of the flow at the downstream region of the nozzle Figure 4 compares the velocity versus radius at two perpendicular rays at a distance downstream of the nozzle. As we expect the flow field in the intermediate chamber near the exit to the pump is not axi-symmetric and Figure 5 shows that the velocity on the line passes through the exit pump and the line perpendicular to that is completely different. But fortunately the particle motion at the downstream of the nozzle is important where the flow field is axi-symmetric and this proves that the

axi-symmetric flow assumption at the nozzle downstream used by Zhang et al. [2], Abouali and Ahmadi [17] and Wang et al. [19] is valid.

Path lines are shown in Figure 6. This figure shows that a sizable recirculation zone occurs behind the focusing element walls.

#### 4.1. Particle Motions

In this section the computational results for the particle motions in

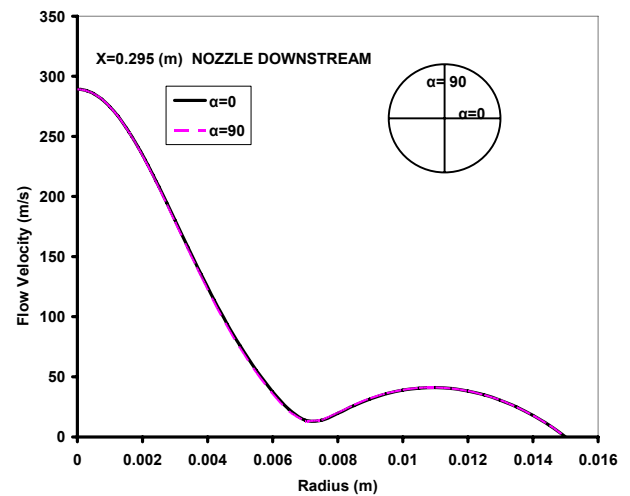


**Figure 4.** Velocity Distribution at 10 mm downstream of the nozzle inside the intermediate chamber for two different circumferential angles.

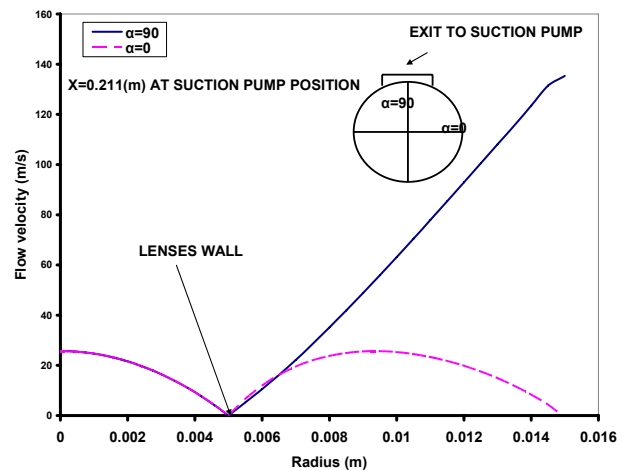


**Figure 5.** Velocity Distribution inside the lens's pipe and intermediate chamber at exit to suction pump location for two different circumferential angles.

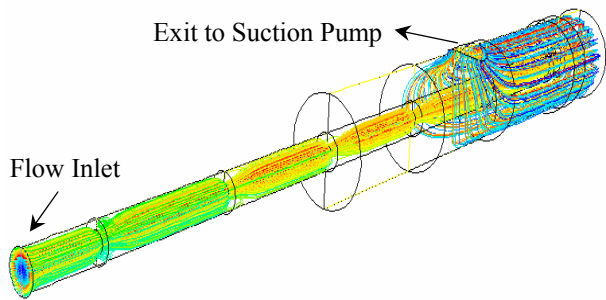


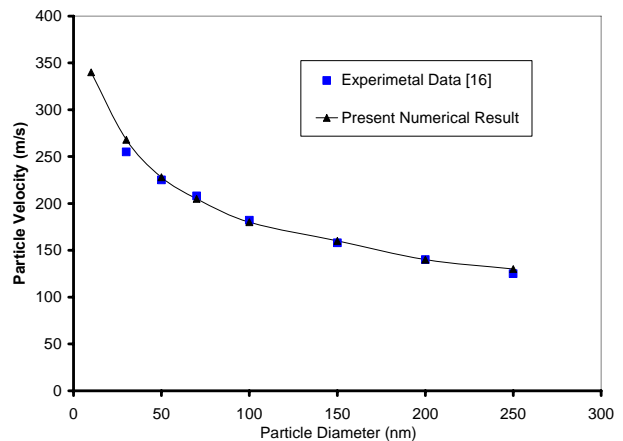
**Figure 6.** Flow path lines inside the aerodynamic lenses and intermediate chamber.

the gas stream are presented. Drag force is the largest force acting on nano- and micro- particles in aerodynamic lens system. The Stokes-Cunningham expression for the drag force is commonly used to include the effect of slip corrections. As noted before, by default a constant Cunningham correction factor can be used in the FLUENT code. The Cunningham slip correction factor depends on the Knudsen number or the gas mean free path. The gas mean free path is a function of the gas pressure (density). When a constant correction factor is used, the mean free path as a function of gas pressure at an appropriate point of the flow needs to be evaluated. A variable Cunningham correction in this study is used [20].

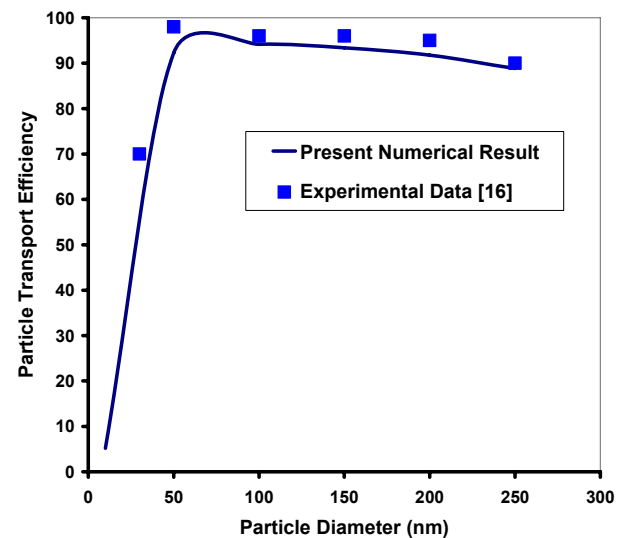
Figure 7 compares the simulation results for particle velocity at different diameters with the experimental data for the large skimmer case. The numerical results accurately duplicate the experimental data in the diameters greater than 30 nm. The particle velocity was calculated at the skimmer exit.

Figure 8 shows the predicted collection efficiency of the aerodynamic lens and the nozzle system. Here the collection efficiency is defined as the ratio of the collected particles in the detection chamber to the number of particles entering the aerodynamic lens system. The experimental data of Liu et al. [16] for the case of the intermediate chamber with a small skimmer is also shown in this figure for comparison. The model prediction appears to be in good agreement with the experimental data and shows that there is an

optimal particle size range for collimation. The decreasing trend of the collection efficiency for particles larger than the optimal size range is due to the impaction of particles on the lens wall. Similarly, for particles smaller than the optimal size range, the Brownian motion increases the dispersion and causes the particles to be trapped on the chamber wall or be carried by the gas into the



**Figure 7.** Comparison of the predicted particle velocities with the experimental data of Liu et al. [16] for different particle diameters for large skimmer case.



**Figure 8.** Comparison of the predicted collection efficiencies of the aerodynamic lens and the nozzle system with the experimental data of Liu et al. [16] for different particle diameters.

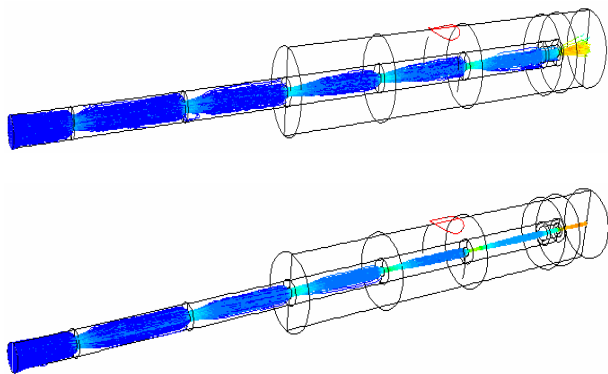
outlet connected to the vacuum pump.

Figure 9 shows sample particles trajectories in the 3-dimensional model of the aerodynamic lens sequence, the nozzle and the intermediate chamber for particle diameters of 10 and 30 nm including the Brownian force. Here the case of a lens with a small skimmer is considered. This figure shows that the Brownian effect reduces the effectiveness of the aerodynamic beam focusing on particles of the order of 10 nm or smaller for the range of pressure condition considered in the present study.

Figure 10 shows the y - direction dispersion of the sub 10 nm particles injected at  $y = 0$  plane at the inlet of the aerodynamic lenses system to emphasize the importance of the 3 - dimensional modeling of the particles motion in this diameter range. If the assumption of the axi-symmetric for particle motion was valid, no particle would have dispersed out of the  $y = 0$  plane. As it can be seen in the figure the particles with 10, 5 and 3 nm diameter dispersed 0.5, 0.75 and 2 mm respectively in y direction inside the lens pipe with a diameter of 5 mm at 25 mm downstream of the pipe inlet. The smaller the particle size, the more the number of them loose in the lenses wall and for 3 nm diameter only two out of ten injected particles reach the 225 mm downstream of the inlet.

## 5. CONCLUSIONS

In the present study, 3-dimensional airflow and



**Figure 9.** Sample simulated 10 nm and 30 nm particle trajectories in the aerodynamic lens system including of Brownian force.

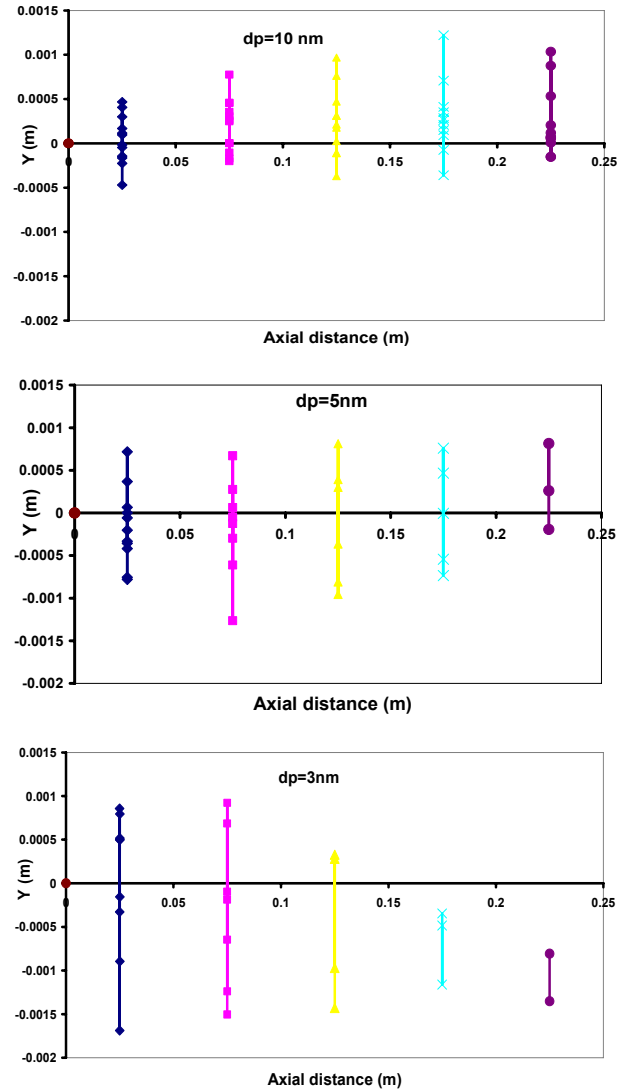


**Figure 10.** Y direction distribution of the 10 particles injected at xz plane at the inlet of the aerodynamic lenses system.

particle motions in a multistage aerodynamic lens with the end nozzle and the intermediate chamber were studied. A variable slip correction factor was used. The simulation results for 3-dimensional flow field show that the assumption of axi-symmetric flow is reasonable at the downstream of the nozzle as used in the literature so far. But the 3-dimensional modeling of the particle motion shows that because of the Brownian motion of sub 10 nm particles, the assumption of the axi-symmetric motion for the particles is not valid and as we expected these particles are highly dispersed

randomly non-symmetrically. It has also been found that the model predictions for collection efficiency and particle velocity are in favorable agreement with the experimental data of Liu et al. [16]. The simulation results show that for particles between a size range of 50 to 1000 nm, a collection efficiency of more than 97 % can be achieved. The collection efficiency for larger particles, however, decreases somewhat due to the inertial impaction effects in the focusing elements. For smaller particles (less than 30 nm), the collection efficiency also decreases due to the Brownian motion effects.

## 6. REFERENCES

- Jayne, J. T., Leard, D. L., Zhang, X., Davidovits, P., Smith, K. A., Kolb, C. E. and Worsnop, D. R., "Development of an Aerosol Mass Spectrometer for Size and Composition Analysis of Submicron Particles", *Aerosol Science and Technology*, Vol. 33, (2000), 49-70.
- Zhang, X., Smith, K. A., Worsnop, D. R., Jimenez, J., Jayne, J. T. and Kolb, C. E., "A Numerical Characterization of Particle Beam Collimation by an Aerodynamic Lens-Nozzle System: Part I. An Individual Lens or Nozzle", *Aerosol Science and Technology*, Vol. 36, (2002), 617-631.
- Kane, D. B. and Johnston, M. V., "Size and Composition Biases on the Detection of Individual Ultrafine Particles by Aerosol Mass Spectrometry", *Environmental Science Technology*, Vol. 34, (2000), 4887-4893.
- Kane, D. B., Oktem, B. and Johnston, M. V., "Nanoparticle Detection by Aerosol Mass Spectrometry", *Aerosol Science and Technology*, Vol. 34, (2001), 520-527.
- Murphy, W. K. and Sears, G. W., "Production of Particles Beams", *Journal of Applied Physics*, Vol. 85, (1964), 1986-1987.
- Dahneke, B. E. and Cheng, Y. S., "Properties of Continuum Source Particle Beam. I. Calculation Method and Results", *Journal of Aerosol Science*, Vol. 10, (1979), 257-274.
- Dahneke, B. E. and Cheng, Y. S., "Properties of Continuum Source Particle Beam. II. Beam Generated in Capillary Expansion", *Journal of Aerosol Science*, Vol. 10, (1979), 257-274.
- Estes, T. J., Vilker, V. L. and Friendlander, S. K., "Characteristics of a Capillary Generated Particle Beam", *Journal of Colloid Interface Science*, Vol. 93, (1983), 84-94.
- Fernandez de la Mora, J. and Riesco - Chueca, P., "Aerodynamic Focusing of Particles in a Carrier Gas", *Journal of Fluid Mechanics*, Vol. 195, (1988), 1-21.
- Israel, G. W. and Freidlander, S. K., "High Speed Beams of Small Particles", *Journal of Colloid Interface Science*, Vol. 24, 330-337.
- Mallina, R. V., Wexler, A. S. and Johnson, M. V., "High Speed Particle Beam Generation: Simple Focusing Mechanisms", *Journal Aerosol Science*. Vol. 30, (1999), 719-738.
- Middha, P. and Wexler, A. S., "Particle Focusing Characteristics of Sonic Jet", *Aerosol Science Technology*, Vol. 37, (2003), 907-915.
- Rao, N. P., Navascues, J. and Fernandez de la Mora, J., "Aerodynamic Focusing of the Particles in Viscous Jets", *Journal of Aerosol Science*, Vol. 24, 879-892.
- Kievit, O., Weiss, M., Verheijet, P. J. T., Marijnissen, J. C. M. and Scarlett, B., "The On-Line Chemical Analysis of Single Particles Using Aerosol Beams and Time of Flight Mass Spectrometer", *Chemical Engineering Communication*, Vol. 151, (1996), 79-100.
- Liu, P., Ziemann, P. L., Kitt elson, D. B. and McMurry, P. H., "Generating Particle Beams of Controlled Dimensions and Divergence: I. Theory of Particle Motion in Aerodynamic Lenses and Nozzle Expansions", *Aerosol Science Technology*, Vol. 22, (1995), 293-313.
- Liu, P., Ziemann, P. L., Kitt elson, D. B. and McMurry, P. H., "Generating Particle Beams of Controlled Dimensions and Divergence: II. Experimental Evaluation of Particle Motion in Aerodynamic Lenses and Nozzle Expansions", *Aerosol Science and Technology*, Vol. 22, (1995), 314-324.
- Abouali, O. and Ahmadi, G., "Numerical Simulation of Supersonic Flow and Particle Motion in Aerodynamic Lenses", *ASME Fluid Engineering Summer Conference*, Honolulu, Hawaii, July, (2003), 7-11.
- Zhang, X., Smith, K. A., Worsnop, D. R., Jimenez, J., Jayne, J. T., Kolb, C. E., Morris, J. and Davidovits, P., "Numerical Characterization of Particle Beam Collimation: Part II Integrated Aerodynamic Lens - Nozzle System", *Aerosol Science Technology*, Vol. 38, (2004), 619-638.
- Wang, X., Gidwani, A., Girshick, S. L. and McMurry, P. H., "Aerodynamic Focusing of Nanoparticles: II. Numerical Simulation of Particle Motion Through Aerodynamic Lenses", *Aerosol Science Technology*, Vol. 39, (2005), 624-636.
- Hinds, W. C., "Aerosol Technology, John Wiley and Sons", Inc., Second Edition, (1999).
- Abouali, O. and Ahmadi, G., "A model for Supersonic and Hypersonic Impactors for Nano - particles", *Journal of Nano-particles*, Vol. 7, No. 1, (2005), 75-88.
- Hering, S. V., Friedlander, S. K., Collins, J. J. and Richards, L. W., "Design and Evaluation of a New Low - Pressure Impactor, Part 2. Environmental", *Science and Technology*, Vol. 13, (1979), 184-188.
- Li, A. and Ahmadi, G., "Deposition of Aerosols on Surfaces in a Turbulent Channel Flow", *International Journal of Engineering Science*, Vol. 31, (1993), 435-445,
- FLUENT Users' Manual, "Discrete Phase Modeling", (1998).